

**Metal Acetylide CpW(CO)<sub>3</sub>C≡CPh and Hydride CpW(CO)<sub>3</sub>H  
Complexes as Building Blocks To Prepare Tungsten-Ruthenium  
Heterometallic Clusters. Synthesis, Characterization, and  
Crystal Structure of CpWRu<sub>3</sub>(CO)<sub>9</sub>(μ<sub>3</sub>-COMe)(C=CHPh),  
Cp<sub>2</sub>W<sub>2</sub>Ru<sub>3</sub>(CO)<sub>9</sub>[CC(Ph)C(OMe)](C=CHPh), and  
Cp<sub>2</sub>W<sub>2</sub>Ru<sub>3</sub>(CO)<sub>9</sub>(COMe)(C≡CPh)**

Yun Chi\* and Shioh-Huey Chuang

*Department of Chemistry, National Tsing Hua University, Hsinchu 30043, Taiwan, Republic of China*

Ling-Kang Liu† and Yuh-Sheng Wen

*Institute of Chemistry, Academia Sinica, Taipei 11529, Taiwan, Republic of China*

Received December 17, 1990

The reaction of the methoxymethylidyne complex HRu<sub>3</sub>(CO)<sub>10</sub>(μ-COMe) (1) and the tungsten acetylide complex CpW(CO)<sub>3</sub>C≡CPh in refluxing toluene produced the vinylidene complex CpWRu<sub>3</sub>(CO)<sub>9</sub>(μ<sub>3</sub>-COMe)(C=CHPh) (2). The fluxionality of the Ru-CO ligands of 2 was studied by variable-temperature <sup>13</sup>C NMR spectroscopy. Further reaction of 2 with the tungsten acetylide CpW(CO)<sub>3</sub>C≡CPh gave another vinylidene complex, Cp<sub>2</sub>W<sub>2</sub>Ru<sub>3</sub>(CO)<sub>9</sub>[CC(Ph)C(OMe)](C=CHPh) (3), whereas reaction with the tungsten hydride CpW(CO)<sub>3</sub>H produced the acetylide complex Cp<sub>2</sub>W<sub>2</sub>Ru<sub>3</sub>(CO)<sub>9</sub>(μ<sub>3</sub>-COMe)(C≡CPh) (4). The structures of complexes 2-4 were determined by X-ray diffraction studies. Crystal data for 2: space group P2<sub>1</sub>/n; a = 8.986 (3) Å, b = 17.577 (3) Å, c = 16.460 (2) Å, β = 94.11 (1)°, Z = 4; final R<sub>F</sub> = 0.021 and R<sub>w</sub> = 0.026 for 4055 reflections with I > 2σ(I). Crystal data for 3: space group P1̄; a = 10.356 (3) Å, b = 10.887 (1) Å, c = 18.121 (2) Å, α = 91.28 (1)°, β = 76.76 (1)°, γ = 110.34 (2)°, Z = 2; final R<sub>F</sub> = 0.024 and R<sub>w</sub> = 0.030 for 5571 reflections with I > 2.5σ(I). Crystal data for 4: space group P2<sub>1</sub>/c, a = 9.850 (1) Å, b = 10.702 (1) Å, c = 30.721 (3) Å, β = 96.597 (1)°, Z = 4; final R<sub>F</sub> = 0.064 and R<sub>w</sub> = 0.070 for 4663 reflections with I > 2σ(I). The most striking structural feature of the Ru<sub>3</sub>W<sub>2</sub> complexes 3 and 4 involves the presence of quadruply bridging vinylidene (μ<sub>4</sub>-η<sup>2</sup>-C=CHPh) and carbonyl (μ<sub>4</sub>-η<sup>2</sup>-CO) ligands, respectively.

The reactivity of mixed-metal clusters has been of interest for many years.<sup>1</sup> Research in this area is stimulated by a belief that the combination of metals having different properties within one molecule may induce unique chemical transformations. In seeking to explore the chemistry of the unsaturated hydrocarbon fragment on the coordination sphere of polynuclear heterometallic complexes, we have examined the reaction between the mononuclear metal acetylide LW(CO)<sub>3</sub>C≡CR and the cluster complexes Os<sub>3</sub>(CO)<sub>10</sub>(CH<sub>3</sub>CN)<sub>2</sub>, Ru<sub>3</sub>(CO)<sub>12</sub>, Ru<sub>3</sub>(CO)<sub>10</sub>(μ<sub>3</sub>-NPh), and LWRu<sub>2</sub>(CO)<sub>8</sub>(μ-H)(μ<sub>3</sub>-NPh) with the goal of searching for a systematic method to prepare the heterometallic clusters required.<sup>2</sup> During our investigation, we found that the imido group (μ<sub>3</sub>-NPh) functioned as a "protecting group" to hold together the metal atoms and to prevent unwanted cluster fragmentation.<sup>3</sup> Therefore, we decided to extend the above reaction to another trinuclear complex with a similar capping group. The triruthenium complex HRu<sub>3</sub>(CO)<sub>10</sub>(μ-COMe) (1) fits well into this category. Furthermore, because the reactions of its triosmium analogue HOs<sub>3</sub>(CO)<sub>10</sub>(μ-COMe) with alkynes and the reaction of H<sub>3</sub>Ru<sub>3</sub>(CO)<sub>9</sub>(μ<sub>3</sub>-COMe) and alkynes have all been well established,<sup>4</sup> our investigation furnished an opportunity, from the viewpoint of organometallic synthesis, to compare the chemistry and reactivity of the organic acetylides RC≡CR' with those of the analogous organometallic acetylide L<sub>n</sub>MC≡CR.

In this paper, we report details of the reaction of 1 with CpW(CO)<sub>3</sub>C≡CPh and the succeeding cluster expansion reactions of the Ru<sub>3</sub>W derivative CpWRu<sub>3</sub>(CO)<sub>9</sub>(μ<sub>3</sub>-COMe)(C=CHPh) (2) derived from this reaction. The

related reaction of 1 with tungsten hydrides LW(CO)<sub>3</sub>H (L = Cp and Cp\*)<sup>5</sup> and the condensation between the anionic cluster [H<sub>2</sub>Ru<sub>3</sub>(CO)<sub>9</sub>(μ<sub>3</sub>-COMe)]<sup>-</sup> and the cationic complex [Rh(CO)<sub>3</sub>(PPh<sub>3</sub>)<sub>2</sub>]<sup>+</sup>PF<sub>6</sub><sup>-</sup> have all been described recently.<sup>6</sup>

### Experimental Procedure

**General Information and Materials.** Infrared spectra were recorded on a Bomen M-100 FT-IR spectrometer. <sup>1</sup>H and <sup>13</sup>C NMR spectra were recorded on a Bruker AM-400 (400.13 MHz) instrument or a Varian Gemini-300 (300 MHz) instrument. Mass spectra were obtained on a JEOL-FX110 instrument operating in the fast atom bombardment (FAB) mode. All reactions were performed under a nitrogen atmosphere with use of deoxygenated solvents dried with an appropriate reagent. The progress of reactions was monitored by analytical thin-layer chromatography (5735 Kieselgel 60 F<sub>254</sub>, E. Merck), and the products were separated on the commercially available preparative thin-layer chromatographic plates (Kieselgel 60 F<sub>254</sub>, E. Merck). The metal acetylide CpW(CO)<sub>3</sub>C≡CPh,<sup>7</sup> the metal hydride CpW(CO)<sub>3</sub>H,<sup>8</sup>

(1) (a) Gladfelter, W. L.; Geoffroy, G. L. *Adv. Organomet. Chem.* 1980, 18, 207. (b) Roberts, D. A.; Geoffroy, G. L. In *Comprehensive Organometallic Chemistry*; Wilkinson, G., Stone, F. G. A., Abel, E. W., Eds.; Pergamon: Oxford, U. K., 1982; Vol. 6, Chapter 40. (c) *The Chemistry of Cluster Complexes*; Shriver, D. F., Keesz, H. D., Adams, R. D., Eds.; VCH Publishers: New York, 1990.

(2) (a) Chi, Y.; Lee, G.-H.; Peng, S.-M.; Wu, C.-H. *Organometallics* 1989, 8, 1574. (b) Chi, Y.; Lee, G.-H.; Peng, S.-M.; Liu, B.-J. *Polyhedron* 1989, 8, 2003. (c) Chi, Y.; Hwang, D.-K.; Chen, S.-F.; Liu, L.-K. *J. Chem. Soc., Chem. Commun.* 1989, 1540. (d) Chi, Y.; Liu, L.-K.; Huttner, G.; Zsolnai, L. *J. Organomet. Chem.* 1990, 390, C50.

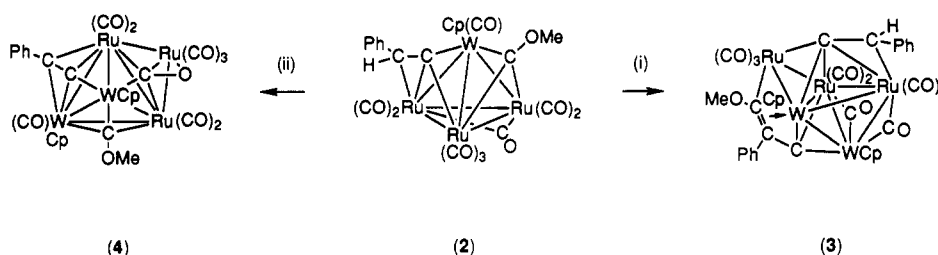
(3) Huttner, G.; Knoll, K. *Angew. Chem., Int. Ed. Engl.* 1987, 26, 743.

(4) (a) Beanan, L. R.; Rahman, Z. A.; Keister, J. B. *Organometallics* 1983, 2, 1062. (b) Beanan, L. R.; Keister, J. B. *Organometallics* 1985, 4, 1713.

(5) Chi, Y.; Chuang, S.-H.; Chen, B.-F.; Peng, S.-M.; Lee, G.-H. *J. Chem. Soc., Dalton Trans.* 1990, 3033.

(6) Evans, J.; Stroud, P. M.; Webster, M. *J. Chem. Soc., Chem. Commun.* 1989, 1029.

† To whom inquiries concerning the X-ray crystallographic work should be addressed.

Scheme I<sup>a</sup>

<sup>a</sup>Legend: (i) with  $\text{CpW}(\text{CO})_3\text{C}\equiv\text{CPh}$ ; (ii) with  $\text{CpW}(\text{CO})_3\text{H}$ .

and the ruthenium methoxymethylidyne  $\text{HRu}_3(\text{CO})_{10}(\mu\text{-COMe})^9$  complexes were prepared according to the literature procedures. Elemental analyses were performed at the NSC Regional Instrument Center at National Cheng Kung University, Tainan, Taiwan.

**Reaction of  $\text{CpW}(\text{CO})_3\text{C}\equiv\text{CPh}$  with  $\text{HRu}_3(\text{CO})_{10}(\mu\text{-COMe})$ .** A toluene solution (40 mL) of a mixture of  $\text{CpW}(\text{CO})_3\text{C}\equiv\text{CPh}$  (325 mg, 0.75 mmol) and  $\text{HRu}_3(\text{CO})_{10}(\mu\text{-COMe})$  (427 mg, 0.68 mmol) was heated at reflux for 30 min, during which time the color of the solution turned from orange to dark green. After evaporation of the solvent on a rotary evaporator, the residue was separated by preparative thin-layer chromatography (1:2 dichloromethane–hexane) and purified by recrystallization, giving 164 mg of the orange starting material  $\text{HRu}_3(\text{CO})_{10}(\mu\text{-COMe})$  (0.26 mmol, 35%) and 251 mg of the olive green vinylidene complex  $\text{CpWRu}_3(\text{CO})_9(\mu_3\text{-COMe})(\text{C}=\text{CHPh})$  (2; 0.264 mmol, 39%). Crystals of 2 suitable for X-ray diffraction were obtained by recrystallization from a layered solution of dichloromethane–heptane at room temperature. Spectral data for 2: MS (FAB,  $^{102}\text{Ru}$ ,  $^{184}\text{W}$ )  $m/z$  956 ( $\text{M}^+$ ); IR ( $\text{C}_6\text{H}_{12}$ )  $\nu(\text{CO})$  2061 (s), 2032 (vs), 2011 (vs), 2001 (m), 1994 (m), 1985 (w), 1955 (w), 1811 (vw, br)  $\text{cm}^{-1}$ ;  $^1\text{H}$  NMR ( $\text{CD}_2\text{Cl}_2$ , 294 K)  $\delta$  7.29 (t, 2 H,  $J_{\text{H-H}} = 7.6$  Hz,  $m$   $\text{C}_6\text{H}_5$ ), 7.21 (t, 1 H,  $J_{\text{H-H}} = 6.9$  Hz,  $p$   $\text{C}_6\text{H}_5$ ), 6.97 (s, 1 H,  $\text{C}=\text{CHPh}$ ), 6.92 (d, 2 H,  $J_{\text{H-H}} = 7.5$  Hz,  $o$   $\text{C}_6\text{H}_5$ ), 5.75 (s, 5 H,  $\text{C}_6\text{H}_5$ ), 4.06 (s, 3 H,  $\text{OCH}_3$ );  $^{13}\text{C}$  NMR ( $\text{CDCl}_3$ , 294 K)  $\delta$  330.5 (COMe,  $J_{\text{C-W}} = 142$  Hz), 256.8 (W–CO,  $J_{\text{C-W}} = 177$  Hz), 208.0 (3 C, br, Ru–CO), 199.9 (1 C, Ru–CO), 194.3 (3 C, Ru–CO), 187.7 (1 C, Ru–CO), 143.6 ( $i$   $\text{C}_6\text{H}_5$ ), 129.4 ( $o,m$   $\text{C}_6\text{H}_5$ ), 128.2 ( $m,o$   $\text{C}_6\text{H}_5$ ), 127.5 ( $p$   $\text{C}_6\text{H}_5$ ), 95.6 ( $\text{C}_5\text{H}_5$ ), 89.4 (C=CHPh), 77.2 (C=CHPh), 25.6 ( $\text{OCH}_3$ ). Anal. Calcd for  $\text{C}_{24}\text{H}_{14}\text{O}_{10}\text{Ru}_3\text{W}$ : C, 30.36; H, 1.49. Found: C, 30.35; H, 1.53.

**Reaction of  $\text{CpWRu}_3(\text{CO})_9(\mu_3\text{-COMe})(\text{C}=\text{CHPh})$  with  $\text{CpW}(\text{CO})_3\text{C}\equiv\text{CPh}$ .** A toluene solution (35 mL) of  $\text{CpWRu}_3(\text{CO})_9(\mu_3\text{-COMe})(\text{C}=\text{CHPh})$  (40 mg, 0.042 mmol) and  $\text{CpW}(\text{CO})_3\text{C}\equiv\text{CPh}$  (20 mg, 0.046 mmol) was heated at reflux for 55 min. The color of the solution turned from olive green to dark brown. After evaporation of the solvent on a rotary evaporator, the residue was separated by preparative thin-layer chromatography (2:3 dichloromethane–hexane) and purified by recrystallization, giving 7.2 mg of the dark brown vinylidene complex  $\text{Cp}_2\text{W}_2\text{Ru}_3(\text{CO})_9[\text{CC}(\text{Ph})\text{C}(\text{OMe})](\text{C}=\text{CHPh})$  (3; 0.0055 mmol, 13%). Crystals of 3 suitable for X-ray diffraction were obtained by recrystallization from a layered solution of dichloromethane–hexane at room temperature. Spectral data for 3: MS (FAB,  $^{102}\text{Ru}$ ,  $^{184}\text{W}$ )  $m/z$  1302 ( $\text{M}^+$ ); IR ( $\text{C}_6\text{H}_{12}$ )  $\nu(\text{CO})$  2057 (s), 2018 (vs), 2003 (vs), 1977 (w), 1967 (m)  $\text{cm}^{-1}$ ;  $^1\text{H}$  NMR ( $\text{CDCl}_3$ , 294 K)  $\delta$  7.52 (d, 2 H,  $J_{\text{H-H}} = 7.8$  Hz,  $o$   $\text{C}_6\text{H}_5$ ), 7.47 (s, 1 H, C=CHPh), 7.45–7.40 (m, 3 H), 7.33 (t, 2 H,  $J_{\text{H-H}} = 7.6$  Hz,  $m$   $\text{C}_6\text{H}_5$ ), 7.19 (t, 1 H,  $J_{\text{H-H}} = 6.9$  Hz,  $p$   $\text{C}_6\text{H}_5$ ), 7.02 (d, br, 2 H,  $J_{\text{H-H}} = 6.9$  Hz,  $o$   $\text{C}_6\text{H}_5$ ), 5.37 (s, 5 H,  $\text{C}_6\text{H}_5$ ), 4.64 (s, 5 H,  $\text{C}_6\text{H}_5$ ), 3.93 (s, 3 H,  $\text{OCH}_3$ ). Anal. Calcd for  $\text{C}_{37}\text{H}_{24}\text{O}_{10}\text{Ru}_3\text{W}_2$ : C, 34.20; H, 1.86. Found: C, 33.42; H, 1.89.

**Reaction of  $\text{CpWRu}_3(\text{CO})_9(\mu_3\text{-COMe})(\text{C}=\text{CHPh})$  with  $\text{CpW}(\text{CO})_3\text{H}$ .** In a 50-mL reaction flask, a solution of  $\text{CpW}(\text{CO})_3\text{H}$  (27 mg, 0.081 mmol) in 10 mL of toluene was added slowly

to a refluxing toluene solution (30 mL) of  $\text{CpWRu}_3(\text{CO})_9(\mu_3\text{-COMe})(\text{C}=\text{CHPh})$  (32 mg, 0.034 mmol) over a period of nearly 60 min. Then, the mixture was continuously refluxed for another 50 min before workup. During this process, the solution turned from olive green to dark brown. After evaporation of the solvent under vacuum, the residue was separated by preparative thin-layer chromatography (2:3 dichloromethane–hexane) and purified by recrystallization, affording 10 mg of red  $\text{Cp}_2\text{W}_2\text{Ru}_3(\text{CO})_9(\mu_3\text{-COMe})(\text{C}=\text{CHPh})$  (4; 0.0082 mmol, 24%). Crystals of 4 suitable for X-ray diffraction were obtained by recrystallization from a layered solution of dichloromethane–methanol at room temperature. Spectral data for 4: MS (FAB,  $^{102}\text{Ru}$ ,  $^{184}\text{W}$ )  $m/z$  1200 ( $\text{M}^+$ ); IR ( $\text{C}_6\text{H}_{12}$ )  $\nu(\text{CO})$  2066 (vs), 2009 (vs), 1999 (vs), 1990 (s), 1976 (vw), 1962 (w), 1942 (m)  $\text{cm}^{-1}$ ;  $^1\text{H}$  NMR ( $\text{CD}_2\text{Cl}_2$ , 294 K)  $\delta$  7.46 (d, 2 H,  $J_{\text{H-H}} = 7.6$  Hz,  $o$   $\text{C}_6\text{H}_5$ ), 7.35 (t, 2 H,  $J_{\text{H-H}} = 7.5$  Hz,  $m$   $\text{C}_6\text{H}_5$ ), 7.21 (t, 1 H,  $J_{\text{H-H}} = 7.5$  Hz,  $p$   $\text{C}_6\text{H}_5$ ), 6.12 (s, 5 H,  $\text{C}_6\text{H}_5$ ), 5.21 (s, 5 H,  $\text{C}_6\text{H}_5$ ), 3.69 (s, 3 H,  $\text{OCH}_3$ ). Anal. Calcd for  $\text{C}_{28}\text{H}_{18}\text{O}_{10}\text{Ru}_3\text{W}_2$ : C, 29.09; H, 1.52. Found: C, 28.47; H, 1.56.

**X-ray Crystallography.** Diffraction measurements of complexes 2 and 3 were carried out on a Nonius CAD-4 diffractometer, and data collection of complex 4 was performed on a Rigaku AFC-5R diffractometer, respectively. Lattice parameters of 2 were determined from 25 randomly selected reflections with  $2\theta$  angles in the range 18.40–32.86°. Lattice parameters of 3 were determined from 25 randomly selected reflections with  $2\theta$  angles in the range 15.25–34.55°, whereas the corresponding lattice parameters of 4 were determined from 20 reflections with  $2\theta$  angles in the range 38.56–57.92°. Intensities were corrected for Lorentz, polarization, and absorption effects. All data reductions and structural refinements were performed with use of the NRCC-SDP-VAX packages.<sup>10</sup> The structures were solved by the heavy-atom method and refined by least-squares cycles; all non-hydrogen atoms were refined with anisotropic thermal parameters. The data collection and refinement parameters for complexes 2–4 are given in Table I. Atomic positional parameters for complex 2 are found in Table II, whereas some selected bond angles and lengths are given in Table III. The corresponding parameters for complexes 3 and 4 are given in Tables IV and V and Tables VI and VII, respectively.

## Results and Discussion

### Synthesis and Characterization of Complex 2.

Treatment of the triruthenium methoxymethylidyne complex  $\text{HRu}_3(\text{CO})_{10}(\mu\text{-COMe})$  (1) with  $\text{CpW}(\text{CO})_3\text{C}\equiv\text{CPh}$  in refluxing toluene yielded the olive green vinylidene mixed-metal cluster  $\text{CpWRu}_3(\text{CO})_9(\mu_3\text{-COMe})(\text{C}=\text{CHPh})$  (2, 39%) in addition to 35% unreacted starting material (Scheme I). The products were easily separated from the starting material and other minor products by preparative thin-layer chromatography. Following further purification by recrystallization we obtained dark green crystalline solids. The formula of 2 was initially determined by FAB mass spectrometry, which indicated a parent ion at  $m/z$  956, corresponding to the composition  $\text{C}_{24}\text{H}_{14}\text{O}_{10}\text{Ru}_3\text{W}$ .

(7) Bruce, M. I.; Humphrey, M. G.; Matisons, J. G.; Roy, S. K.; Swincer, A. G. *Aust. J. Chem.* 1984, 37, 1955.

(8) Braunstein, P.; Bender, R.; Jud, J. *Inorg. Synth.* 1989, 26, 341.

(9) Keister, J. B.; Payne, M. W.; Muscatella, M. J. *Organometallics* 1983, 2, 219.

(10) Gabe, E. J.; Lee, F. L.; Le Page, Y. In *Crystallographic Computing 3: Data Collection, Structure Determination, Proteins, and Data Bases*; Sheldrick, G. M., Krueger, C., Goddard, R., Eds.; Clarendon Press: Oxford, U.K., 1985; pp 167–174.

Table I. Experimental Data for the X-ray Diffraction Analysis of Complexes 2-4

compd	2	3	4
formula	C <sub>24</sub> H <sub>14</sub> O <sub>10</sub> Ru <sub>3</sub> W	C <sub>37</sub> H <sub>24</sub> O <sub>10</sub> Ru <sub>3</sub> W <sub>2</sub> (solvate) <sup>a</sup>	C <sub>28</sub> H <sub>18</sub> O <sub>10</sub> Ru <sub>3</sub> W <sub>2</sub> ·H <sub>2</sub> O
mol wt	949.42	1299.50 + solvate	1215.38
cryst syst	monoclinic	triclinic	monoclinic
space group	P2 <sub>1</sub> /n	P1	P2 <sub>1</sub> /c
a, Å	8.986 (3)	10.356 (3)	9.850 (1)
b, Å	17.577 (3)	10.887 (1)	10.702 (1)
c, Å	16.460 (2)	18.121 (2)	30.721 (3)
α, deg		91.28 (1)	
β, deg	94.11 (1)	76.76 (1)	96.597 (1)
γ, deg		110.34 (2)	
V, Å <sup>3</sup>	2593 (1)	1861 (1)	3217 (1)
Z	4	2	4
D <sub>x</sub> , g/cm <sup>3</sup>	2.43	2.33 + solvate	2.50
F(000)	1775.65	1211.71 + solvate	2247.44
diffractometer	Nonius (CAD-4)	Nonius (CAD-4)	Rigaku (AFC-5R)
radiation, Å	λ(Mo Kα) = 0.709 30	λ(Mo Kα) = 0.709 30	λ(Cu Kα) = 1.540 56 Å
temp, K	297	297	297
scan method	θ/2θ scan mode	θ/2θ scan mode	θ/2θ scan mode
2θ(max), deg	50	50	120
hkl ranges	-10 to +10, 0-20, 0-19	-12 to +11, 0-12, -21 to +21	-11 to +11, 0-12, 0-34
cryst size, mm	0.44 × 0.16 × 0.20	0.27 × 0.19 × 0.09	0.42 × 0.12 × 0.18
μ, mm <sup>-1</sup>	6.25	7.51	24.97
transmission factors: min, max	0.855, 1.000	0.594, 1.000	0.541, 1.00
no. of unique rflns	4551, 4055 with I > 2σ(I)	6547, 5571 with I > 2.5σ(I)	4777, 4663 with I > 2σ(I)
weighting scheme	based on counting statistics	based on counting statistics	counting statistic weights
fudge factor	0.001	0.01	0.03
no. of atoms and params	52, 344	79, 496	63, 407
max Δ/σ ratio	0.049	0.045	0.020
R <sub>F</sub> ; R <sub>w</sub> <sup>b</sup>	0.021; 0.026	0.024; 0.030	0.064; 0.070
GOF <sup>b</sup>	1.46	1.52	1.44
max/min residual electron density, e Å <sup>-3</sup>	0.73/-0.85	0.65/-1.11	4.93/-4.38 <sup>c</sup>

<sup>a</sup>The solvate molecule may be a disordered CH<sub>2</sub>Cl<sub>2</sub> or hexane molecule; no appropriate model(s) could be derived. <sup>b</sup>R<sub>F</sub> = Σ|F<sub>o</sub> - F<sub>c</sub>|/Σ|F<sub>o</sub>|; R<sub>w</sub> = [Σw|F<sub>o</sub> - F<sub>c</sub>|<sup>2</sup>/Σw|F<sub>o</sub>|<sup>2</sup>]<sup>1/2</sup>; GOF = [Σw|F<sub>o</sub> - F<sub>c</sub>|<sup>2</sup>/(N<sub>o</sub> - N<sub>v</sub>)]<sup>1/2</sup> (N<sub>o</sub> = number of observations; N<sub>v</sub> = number of variables). <sup>c</sup>The largest residual peaks were found to be around the Ru and W atoms within the range 1.00-1.20 Å.

This result suggests that the formation of 2 involves a condensation of the triruthenium cluster complex 1 with one CpW(CO)<sub>3</sub>C≡CPh molecule accompanied by elimination of four CO ligands. The <sup>1</sup>H NMR spectrum shows a signal at δ 6.97, in addition to the respective signals assigned to the phenyl, methoxy, and Cp groups. The observation of this downfield singlet suggests that the acetylide ligand of CpW(CO)<sub>3</sub>C≡CPh has coupled with the bridging hydride of 1 to afford the vinylidene (C=CHPh) group during the reaction. Consistent with this assignment, the <sup>13</sup>C NMR spectrum exhibited two signals at δ 89.4 and 77.2, which are assigned to the vinylidene α- and β-carbons, respectively. The chemical shift of the α-carbon is substantially different from the NMR chemical shift data summarized in the literature.<sup>11</sup> Although the cause of the abnormal high-field shift is not understood, we speculate it may be related to the unsaturated behavior of this complex in solution (vide infra). Finally, the IR spectrum of 2 in the region of CO stretching absorptions exhibits peaks due to terminal CO ligands at 2061, 2032, 2011, 2001, 1994, 1985, and 1955 cm<sup>-1</sup> and a weak absorption at 1811 cm<sup>-1</sup> assigned to a bridging CO ligand.

**Crystal Structure of Complex 2.** Dark green, air-stable, brick-shaped crystals were obtained from a layered solution of dichloromethane-hexane at room temperature, and an X-ray diffraction analysis was carried out to establish the exact geometry. The molecular structure and the atomic numbering scheme of 2 are presented in Figure 1. Selected parameters of bond lengths and angles are summarized in Table II. As indicated in Figure 1, the molecule has a tetrahedral WRu<sub>3</sub> core arrangement in which the tungsten atom is coordinated to a Cp ring and a terminal CO ligand. The ruthenium atom Ru(3) is associated with three terminal CO ligands, whereas the atoms

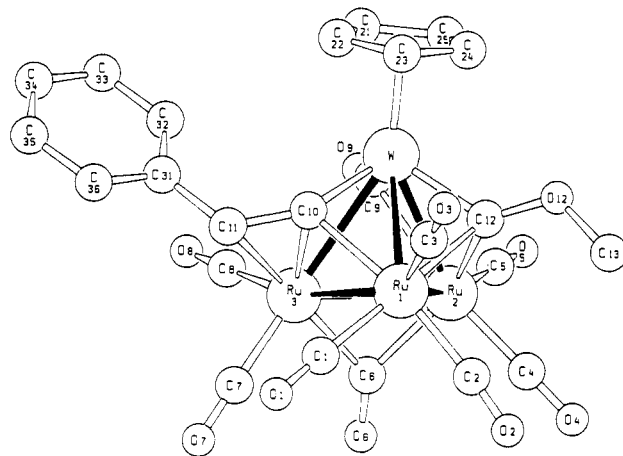


Figure 1. Molecular structure of CpWRu<sub>3</sub>(CO)<sub>9</sub>(μ<sub>3</sub>-COMe)(C=CHPh) (2).

Ru(1) and Ru(2) are each connected to two terminal CO ligands and one bridging CO ligand. All metal-metal bonding interactions are normal, showing metal-metal single-bond lengths in the range 2.7507-2.9730 Å and bond angles ∠M-M-M in the range 58.00-64.55°. The CO ligands on the ruthenium atoms are linear, but the W-CO ligand is slightly bent, with angle ∠W-C(9)-O(9) = 160.9 (4)°. There is a unique bridging CO ligand that bridges the Ru(2)-Ru(3) edge with distances Ru(2)-C(6) = 2.047 (5) Å and Ru(3)-C(6) = 2.134 (5) Å. This Ru(2)-Ru(3) vector is the shortest metal-metal bond of the molecule.

Furthermore, the methoxymethylidyne moiety (μ<sub>3</sub>-COMe) coordinates to the triangular face defined by the atoms Ru(1), Ru(3), and W, with bond lengths W-C(10) = 1.973 (5) Å, Ru(1)-C(10) = 2.191 (4) Å, and Ru(3)-C(10) = 2.122 (4) Å. The methyl substituent is tilted away from the W atom with angle ∠C(12)-O(12)-C(13) = 120.8 (4)°,

Table II. Final Fractional Coordinates for Complex 2

atom	x	y	z	$B_{iso}, \text{\AA}^2$
W	0.98856 (2)	0.18090 (1)	0.06932 (1)	2.25 (1)
Ru(1)	0.76369 (4)	0.21452 (2)	0.17460 (2)	2.22 (2)
Ru(2)	0.98768 (5)	0.10427 (2)	0.21950 (2)	2.53 (2)
Ru(3)	1.05554 (4)	0.25675 (2)	0.22921 (2)	2.16 (1)
O(1)	0.6921 (4)	0.3587 (2)	0.2691 (2)	4.2 (2)
O(2)	0.5751 (5)	0.1329 (2)	0.2949 (3)	5.7 (2)
O(3)	0.5131 (5)	0.2387 (3)	0.0422 (3)	5.7 (2)
O(4)	0.8179 (6)	0.0021 (3)	0.3288 (3)	6.1 (2)
O(5)	1.2067 (6)	-0.0253 (3)	0.2163 (3)	6.2 (2)
O(6)	1.0855 (5)	0.1633 (2)	0.3882 (2)	4.8 (2)
O(7)	1.0102 (5)	0.3577 (2)	0.3741 (2)	5.6 (2)
O(8)	1.3846 (4)	0.2937 (3)	0.2378 (3)	5.6 (2)
O(9)	1.3061 (4)	0.1353 (2)	0.1408 (2)	4.5 (2)
O(12)	0.7520 (4)	0.0563 (2)	0.0772 (2)	3.6 (2)
C(1)	0.7220 (5)	0.3063 (3)	0.2346 (3)	2.9 (2)
C(2)	0.6474 (6)	0.1590 (3)	0.2483 (3)	3.5 (2)
C(3)	0.6039 (6)	0.2290 (3)	0.0918 (3)	3.4 (2)
C(4)	0.8816 (7)	0.0406 (3)	0.2870 (3)	3.9 (3)
C(5)	1.1233 (7)	0.0237 (3)	0.2171 (3)	4.0 (2)
C(6)	1.0609 (6)	0.1684 (3)	0.3182 (3)	3.2 (2)
C(7)	1.0261 (6)	0.3204 (3)	0.3191 (3)	3.3 (2)
C(8)	1.2603 (6)	0.2803 (3)	0.2352 (3)	3.2 (2)
C(9)	1.1801 (6)	0.1505 (3)	0.1280 (3)	3.4 (2)
C(10)	0.9347 (5)	0.2796 (3)	0.1163 (3)	2.4 (2)
C(11)	0.9776 (5)	0.3540 (3)	0.1389 (3)	2.5 (2)
C(12)	0.8367 (5)	0.1111 (3)	0.1132 (3)	2.7 (2)
C(13)	0.6293 (7)	0.0252 (3)	0.1160 (4)	4.9 (3)
C(21)	1.1231 (7)	0.1911 (5)	-0.0454 (3)	5.5 (4)
C(22)	1.0120 (9)	0.2445 (4)	-0.0544 (3)	5.1 (3)
C(23)	0.8778 (8)	0.2067 (5)	-0.0598 (3)	5.5 (4)
C(24)	0.9023 (9)	0.1297 (4)	-0.0572 (3)	5.4 (3)
C(25)	1.0551 (9)	0.1164 (4)	-0.0460 (3)	5.4 (3)
C(31)	1.0929 (5)	0.4010 (3)	0.1021 (3)	2.5 (2)
C(32)	1.2140 (6)	0.3716 (3)	0.0653 (3)	3.7 (2)
C(33)	1.3157 (7)	0.4194 (4)	0.0308 (4)	4.8 (3)
C(34)	1.2968 (7)	0.4966 (4)	0.0339 (4)	4.8 (3)
C(35)	1.1772 (7)	0.5269 (3)	0.0707 (4)	4.6 (3)
C(36)	1.0761 (6)	0.4790 (3)	0.1053 (3)	3.3 (2)

Table III. Selected Bond Distances (Å) and Angles (deg) for Complex 2 (Esds in Parentheses)

(A) Intermetallic Distances and Angles			
W-Ru(1)	2.8173 (8)	W-Ru(2)	2.8156 (5)
W-Ru(3)	2.9730 (5)	Ru(1)-Ru(2)	2.8531 (8)
Ru(1)-Ru(3)	2.811 (1)	Ru(2)-Ru(3)	2.7507 (7)
$\angle$ Ru(1)-Wu-Ru(2)	60.86 (2)	$\angle$ Ru(1)-W-Ru(3)	58.00 (2)
$\angle$ Ru(2)-W-Ru(3)	56.67 (2)	$\angle$ Ru(1)-Ru(3)-Ru(2)	61.72 (1)
$\angle$ W-Ru(1)-Ru(2)	59.54 (2)	$\angle$ W-Ru(1)-Ru(3)	63.78 (2)
$\angle$ Ru(2)-Ru(1)-Ru(3)	58.11 (2)	$\angle$ W-Ru(2)-Ru(1)	59.60 (2)
$\angle$ W-Ru(2)-Ru(3)	64.55 (2)	$\angle$ Ru(1)-Ru(2)-Ru(3)	60.17 (2)
$\angle$ W-Ru(3)-Ru(1)	58.22 (2)	$\angle$ W-Ru(3)-Ru(2)	58.78 (2)
(B) Selected Parameters for the Carbonyl Ligands			
Ru(1)-C(1)	1.942 (5)	Ru(1)-C(2)	1.923 (5)
Ru(1)-C(3)	1.925 (6)	Ru(2)-C(4)	1.884 (6)
Ru(2)-C(5)	1.871 (6)	Ru(2)-C(6)	2.047 (5)
Ru(3)-C(6)	2.134 (5)	Ru(3)-C(7)	1.888 (6)
Ru(3)-C(8)	1.882 (5)	W-C(9)	1.986 (5)
$\angle$ Ru(1)-C(1)-O(1)	177.3 (4)	$\angle$ Ru(1)-C(2)-O(2)	173.3 (5)
$\angle$ Ru(1)-C(3)-O(3)	178.0 (5)	$\angle$ Ru(2)-C(4)-O(4)	179.3 (5)
$\angle$ Ru(2)-C(5)-O(5)	179.4 (5)	$\angle$ Ru(2)-C(6)-O(6)	140.7 (4)
$\angle$ Ru(3)-C(6)-O(6)	136.9 (4)	$\angle$ (3)-C(7)-O(7)	178.7 (5)
$\angle$ Ru(3)-C(8)-O(8)	178.8 (5)	$\angle$ W-C(9)-O(9)	160.9 (4)
(C) Parameters Associated with the Methylidyne Fragment			
W-C(10)	1.973 (5)	Ru(1)-C(10)	2.191 (4)
Ru(3)-C(10)	2.122 (4)		
(D) Parameters Associated with the Vinylidene Fragment			
Ru(3)-C(11)	2.340 (5)	W-C(12)	2.008 (5)
Ru(1)-C(12)	2.203 (5)	Ru(2)-C(12)	2.140 (5)

presumably due to the consequence of minimizing the unfavorable steric interaction with the CpW(CO) vertex. In general, the arrangement and the parameters associated with this triply bridging methylidyne group are similar to

Table IV. Final Fractional Coordinates for Complex 3

atom	x	y	z	$B_{iso}, \text{\AA}^2$
W(1)	0.69910 (3)	0.97750 (3)	0.14521 (1)	2.38 (1)
W(2)	0.58981 (2)	0.78237 (2)	0.28769 (1)	1.89 (1)
Ru(1)	0.85539 (5)	0.83888 (5)	0.18807 (2)	2.01 (2)
Ru(2)	0.81572 (5)	1.04063 (5)	0.27556 (3)	2.48 (2)
Ru(3)	0.74938 (5)	0.61412 (5)	0.28103 (3)	2.25 (2)
O(1)	1.1667 (5)	0.9437 (6)	0.1932 (3)	5.3 (3)
O(2)	0.9156 (6)	0.6749 (6)	0.0546 (3)	5.0 (3)
O(3)	1.0249 (5)	1.1109 (5)	0.0893 (3)	4.4 (2)
O(4)	1.1067 (7)	1.2481 (7)	0.2413 (4)	8.2 (4)
O(5)	0.7161 (8)	1.2119 (7)	0.3912 (4)	7.2 (4)
O(6)	0.5498 (5)	1.1167 (5)	0.2673 (3)	4.1 (3)
O(7)	0.5879 (6)	0.4342 (6)	0.4234 (3)	5.4 (3)
O(8)	1.0330 (6)	0.6949 (6)	0.3279 (3)	5.4 (3)
O(9)	0.8247 (7)	0.4195 (6)	0.1725 (3)	6.2 (3)
O(10)	0.4446 (4)	0.4707 (4)	0.2704 (2)	3.1 (2)
C(1)	1.0495 (7)	0.9038 (7)	0.1914 (3)	3.0 (3)
C(2)	0.8919 (7)	0.7377 (7)	0.1037 (4)	3.0 (3)
C(3)	0.9110 (7)	1.0435 (7)	0.1229 (4)	3.4 (3)
C(4)	0.9980 (9)	1.1696 (8)	0.2536 (4)	4.6 (4)
C(5)	0.7546 (8)	1.1472 (8)	0.3471 (4)	4.2 (4)
C(6)	0.6281 (7)	1.0663 (7)	0.2365 (4)	3.2 (3)
C(7)	0.6463 (7)	0.4976 (7)	0.3693 (4)	3.4 (4)
C(8)	0.9268 (7)	0.6661 (7)	0.3131 (4)	3.3 (3)
C(9)	0.7989 (7)	0.4930 (7)	0.2134 (4)	3.7 (4)
C(10)	0.5667 (6)	0.5810 (6)	0.2415 (3)	2.5 (3)
C(11)	0.4559 (8)	0.3449 (7)	0.2516 (4)	4.2 (4)
C(12)	0.6442 (6)	0.7848 (6)	0.1691 (3)	2.4 (3)
C(13)	0.5477 (6)	0.6560 (6)	0.1834 (3)	2.2 (3)
C(14)	0.7834 (6)	0.8349 (6)	0.3088 (3)	2.3 (3)
C(15)	0.8716 (6)	0.9233 (6)	0.3519 (3)	2.3 (3)
C(21)	0.5218 (8)	0.9907 (10)	0.0899 (4)	4.8 (5)
C(22)	0.5878 (10)	0.9159 (8)	0.0461 (4)	4.9 (5)
C(23)	0.7282 (9)	0.9948 (11)	0.0148 (4)	5.0 (5)
C(24)	0.7462 (9)	1.1198 (9)	0.0413 (5)	5.2 (5)
C(25)	0.6216 (10)	1.1171 (9)	0.0860 (4)	4.9 (5)
C(31)	0.3443 (6)	0.6850 (7)	0.3375 (4)	3.1 (3)
C(32)	0.4144 (7)	0.6628 (7)	0.3918 (4)	3.5 (3)
C(33)	0.840 (7)	0.847 (8)	0.4183 (3)	3.5 (3)
C(34)	0.4641 (7)	0.8841 (7)	0.3778 (4)	3.4 (3)
C(35)	0.3781 (6)	0.8239 (7)	0.3285 (3)	3.0 (3)
C(41)	0.4185 (6)	0.6080 (6)	0.1506 (3)	2.6 (3)
C(42)	0.4055 (8)	0.5040 (8)	0.1053 (4)	4.4 (4)
C(43)	0.2941 (10)	0.4618 (10)	0.0698 (5)	6.2 (5)
C(44)	0.1922 (9)	0.5191 (10)	0.0817 (5)	5.7 (5)
C(45)	0.2079 (8)	0.6235 (9)	0.1245 (4)	4.7 (4)
C(46)	0.3181 (7)	0.6673 (7)	0.1598 (4)	3.5 (3)
C(51)	0.8305 (6)	0.9248 (7)	0.4367 (3)	2.7 (3)
C(52)	0.7688 (7)	0.8090 (7)	0.4817 (3)	3.2 (3)
C(53)	0.2597 (8)	1.1905 (7)	0.4394 (4)	3.9 (4)
C(54)	0.2258 (8)	1.0743 (8)	0.4054 (4)	3.9 (4)
C(55)	0.1643 (7)	0.9610 (7)	0.4491 (4)	3.6 (3)
C(56)	0.8659 (7)	1.0425 (6)	0.4734 (3)	2.9 (3)
C(61) <sup>a</sup>	0.0692 (13)	0.4210 (11)	0.4725 (8)	7.0 (7)
C(62) <sup>a</sup>	-0.0450 (20)	0.4319 (12)	0.4779 (8)	10.3 (11)
C(63) <sup>a</sup>	0.0463 (11)	0.4111 (8)	0.4110 (7)	6.6 (5)

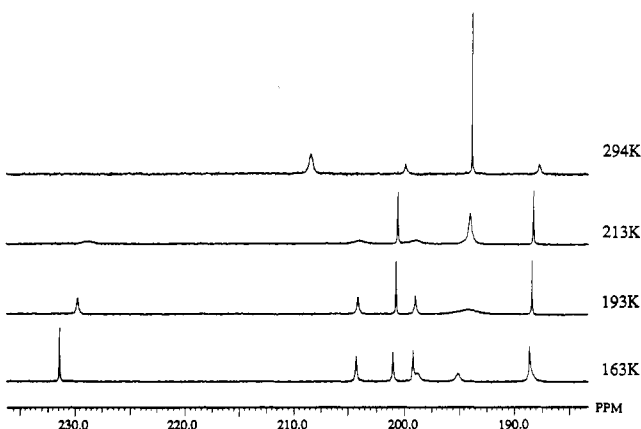
<sup>a</sup> C61-C63 indicate the location of the atoms of the solvate molecule.

those of the methylidyne group in the related, structurally characterized Os<sub>3</sub>W derivative Cp\*WOs<sub>3</sub>(CO)<sub>11</sub>(μ<sub>3</sub>-COMe).<sup>5</sup>

The second hydrocarbon fragment in this molecule is a vinylidene group (C=CHPh), which is derived from the acetylide ligand of CpW(CO)<sub>3</sub>C≡CPh. This fragment is found to be associated with another WRu<sub>2</sub> face defined by the atoms W, Ru(1), and Ru(3). The α-carbon, C(10), is bound to all three metal atoms with W-C(10) = 1.973 (5) Å, Ru(1)-C(10) = 2.191 (4) Å, and Ru(3)-C(10) = 2.122 (4) Å, and the β-carbon, C(11), is linked to atom Ru(1) with Ru(3)-C(11) = 2.340 (5) Å, indicating that the vinylidene ligand is σ-bonded to the atoms W and Ru(3) and π-bonded to the atom Ru(1) via an η<sup>2</sup> interaction. This type of bonding interaction is common; many instances involving the group 8 cluster derivatives have been published in the literature.<sup>12</sup>

**Table V. Selected Bond Distances (Å) and Angles (deg) for Complex 3 (Esd's in Parentheses)**

(A) Intermetallic Distances			
W(1)-W(2)	3.1138 (6)	W(1)-Ru(1)	2.7977 (7)
W(1)-Ru(2)	2.9730 (5)	W(2)-Ru(1)	2.7930 (9)
W(2)-Ru(2)	2.9404 (9)	Ru(1)-Ru(2)	2.7711 (8)
W(2)-Ru(3)	2.8469 (7)	Ru(1)-Ru(3)	2.7388 (8)
(B) Selected Parameters for the Carbonyl Ligands			
Ru(1)-C(1)	1.900 (7)	Ru(1)-C(2)	1.909 (7)
Ru(1)-C(3)	2.367 (7)	Ru(2)-C(4)	1.879 (8)
Ru(2)-C(5)	1.870 (8)	Ru(2)-C(6)	2.317 (7)
Ru(3)-C(7)	1.917 (7)	Ru(3)-C(8)	1.946 (7)
Ru(3)-C(9)	1.901 (7)	W(1)-C(3)	2.001 (7)
W(1)-C(6)	2.019 (7)		
$\angle$ Ru(1)-C(1)-O(1)	179.6 (6)	$\angle$ Ru(1)-C(2)-O(2)	177.7 (6)
$\angle$ Ru(1)-C(3)-O(3)	125.6 (5)	$\angle$ Ru(2)-C(4)-O(4)	178.9 (8)
$\angle$ Ru(2)-C(5)-O(5)	179.5 (8)	$\angle$ Ru(2)-C(6)-O(6)	128.6 (5)
$\angle$ Ru(3)-C(7)-O(7)	176.6 (6)	$\angle$ Ru(3)-C(8)-O(8)	176.3 (6)
$\angle$ Ru(3)-C(9)-O(9)	178.0 (7)	$\angle$ W(1)-C(3)-O(3)	153.4 (5)
$\angle$ W(1)-C(6)-O(6)	149.6 (6)		
(C) Parameters Associated with the C <sub>3</sub> Fragment			
W(2)-C(10)	2.282 (6)	Ru(3)-C(10)	2.088 (6)
W(1)-C(12)	2.002 (6)	Ru(1)-C(12)	2.165 (6)
W(2)-C(12)	2.091 (6)	W(2)-C(13)	2.344 (6)
C(12)-C(13)	1.398 (8)	C(10)-C(13)	1.434 (8)
(D) Parameters Associated with the Vinylidene Fragment			
W(2)-C(14)	2.009 (6)	Ru(1)-C(14)	2.139 (5)
Ru(2)-C(14)	2.222 (6)	Ru(3)-C(14)	2.365 (6)
Ru(2)-C(15)	2.201 (6)	C(14)-C(15)	1.434 (8)
$\angle$ Ru(2)-C(14)-Ru(3)	152.1 (3)	$\angle$ W(2)-C(14)-Ru(3)	80.8 (2)
$\angle$ Ru(3)-C(14)-C(15)	131.9 (4)		

**Figure 2.** Variable-temperature  $^{13}\text{C}$  NMR spectra of **2** in  $\text{CD}_2\text{Cl}_2$ , showing the region of ruthenium CO resonances.

**Fluxionality of the CO Ligands.** Having established the solid-state structure of **2**, we now discuss the exchange motion of the CO ligands. The  $^{13}\text{C}$  NMR spectrum of a  $^{13}\text{CO}$ -enriched sample of **2** at 294 K revealed two downfield signals at  $\delta$  330.5 and 256.8, exhibiting a set of characteristic tungsten satellites with coupling constants  $J_{\text{C-W}} = 142$  and 177 Hz, respectively. The former is assigned to the  $\alpha$ -carbon of the methylidyne group ( $\mu_3$ -COMe) and the latter to the CO ligand associated with the tungsten atom.

For the spectrum recorded at 163 K, we observed eight additional CO signals at  $\delta$  231.3, 204.3, 201.1, 199.2, 198.9,

**Table VI. Final Fractional Coordinates for Complex 4**

atom	x	y	z	$B_{\text{iso}}, \text{\AA}^2$
W(1)	0.21631 (7)	0.94902 (7)	0.17767 (2)	2.02 (3)
W(2)	0.31872 (7)	0.90420 (7)	0.09434 (2)	2.00 (3)
Ru(1)	0.27989 (13)	0.70359 (12)	0.15321 (4)	2.14 (5)
Ru(2)	1.05331 (13)	0.81875 (13)	0.10839 (4)	2.30 (5)
Ru(3)	1.10392 (15)	0.56503 (14)	0.09692 (4)	3.04 (6)
O(1)	0.0313 (16)	0.7721 (16)	0.2247 (5)	5.2 (8)
O(2)	0.2265 (13)	0.6518 (12)	0.0525 (4)	3.2 (5)
O(3)	0.5118 (20)	0.5305 (20)	0.1404 (7)	7.7 (11)
O(4)	0.2417 (21)	0.5474 (18)	0.2323 (5)	7.0 (10)
O(5)	0.9084 (22)	0.8344 (23)	0.0167 (6)	8.5 (12)
O(6)	0.7887 (16)	0.7418 (21)	0.1425 (7)	7.6 (11)
O(7)	0.9543 (20)	0.4825 (19)	0.1715 (6)	6.9 (10)
O(8)	0.8633 (23)	0.5126 (25)	0.0294 (7)	9.0 (13)
O(9)	1.2387 (24)	0.3102 (19)	0.0948 (8)	8.0 (12)
O(10)	0.5344 (11)	0.8787 (13)	0.1733 (4)	3.0 (6)
C(1)	0.1008 (21)	0.8245 (19)	0.2039 (6)	3.5 (9)
C(2)	0.2369 (17)	0.7413 (18)	0.0789 (5)	2.6 (7)
C(3)	0.4251 (23)	0.5960 (20)	0.1452 (6)	3.9 (9)
C(4)	0.2539 (20)	0.6118 (21)	0.2023 (5)	3.5 (9)
C(5)	0.9622 (20)	0.8289 (22)	0.0515 (7)	4.0 (9)
C(6)	0.8906 (23)	0.7733 (25)	0.1288 (7)	4.8 (11)
C(7)	1.0134 (23)	0.5168 (23)	0.1446 (7)	4.3 (10)
C(8)	0.9552 (26)	0.5275 (28)	0.0543 (8)	5.6 (12)
C(9)	1.1911 (27)	0.4056 (24)	0.0958 (8)	5.0 (11)
C(10)	0.4026 (15)	0.8677 (18)	0.1551 (5)	2.5 (7)
C(11)	0.5780 (20)	0.8075 (21)	0.2121 (6)	3.8 (9)
C(12)	1.1555 (17)	0.0025 (17)	0.1082 (5)	2.5 (7)
C(13)	1.0530 (16)	0.0161 (16)	0.1293 (5)	2.3 (7)
C(21)	0.9327 (18)	0.0976 (18)	0.1287 (7)	3.5 (9)
C(22)	0.8946 (22)	0.1755 (20)	0.0929 (8)	4.6 (11)
C(23)	0.7867 (25)	0.2533 (22)	0.0920 (11)	6.0 (14)
C(24)	0.7108 (26)	0.2605 (25)	0.1275 (11)	6.1 (14)
C(25)	0.7422 (25)	0.1843 (28)	0.1631 (10)	6.0 (13)
C(26)	0.8510 (20)	0.1026 (23)	0.1636 (7)	4.5 (10)
C(31)	0.1686 (26)	0.0726 (25)	0.2366 (8)	5.1 (12)
C(32)	0.1889 (29)	0.1521 (20)	0.2028 (7)	4.8 (12)
C(33)	0.3216 (28)	0.1418 (22)	0.1947 (7)	4.6 (11)
C(34)	0.3853 (24)	0.0544 (28)	0.2224 (10)	5.8 (13)
C(35)	0.2914 (38)	0.0110 (22)	0.2479 (7)	6.2 (15)
C(41)	0.4037 (27)	0.8921 (32)	0.0263 (7)	5.5 (13)
C(42)	0.3685 (26)	1.0172 (39)	0.0340 (10)	7.3 (17)
C(43)	0.4543 (31)	1.0589 (26)	0.0695 (10)	6.0 (14)
C(44)	0.5386 (22)	0.9615 (36)	0.0827 (6)	5.6 (15)
C(45)	0.5127 (29)	0.8664 (25)	0.0588 (11)	6.0 (15)
O(11)	0.4746 (20)	0.4031 (22)	0.0279 (6)	8.5 (12)

195.2, 188.6, and 187.9 in the region of ruthenium CO resonances (Figure 2). Because the last two signals at  $\delta$  188.6 and 187.9 are so close to each other, they appeared as a broad, asymmetric signal. The signal at  $\delta$  231.3 is assigned to the bridging CO ligand because its chemical shift is more downfield than the others. When the temperature was raised to 193 K, the signals at  $\delta$  198.9, 195.2, and 187.9 coalesced to form a broad signal at  $\delta$  194.2, which in turn becomes a very sharp signal when the temperature was further increased to 294 K. Therefore, these three signals must be due to the CO ligands of the unique Ru(CO)<sub>3</sub> vertex, which undergoes rapid, localized 3-fold rotation.

Furthermore, as observed in the spectrum recorded at 193 K, there are three relatively broad signals at  $\delta$  231.3, 204.3, and 199.2, which undergo rapid exchange to give a broad signal at  $\delta$  208.0 on warming to 294 K. This motion may be explained in terms of the exchange between the bridging CO and the CO ligands of an adjacent Ru(CO)<sub>2</sub> unit. Interestingly, the exchange with the second Ru(CO)<sub>2</sub> unit was slow in comparison with this process, because the CO signals at  $\delta$  200.7 and 288.2, due to the second Ru(CO)<sub>2</sub> unit, remain very sharp even at 213 K. However, while the temperature was increased to 294 K, the exchange between all five CO ligands coordinated to the atoms Ru(2) and Ru(3) began to take place. The detection of three fairly broad signals at  $\delta$  208.0, 199.9, and 187.7 in the ratio

(12) (a) Deeming, A. J.; Underhill, M. J. *Chem. Soc., Dalton Trans.* 1974, 1415. (b) Chi, Y.; Chen, B.-F.; Wang, S.-L.; Chiang, R.-K.; Hwang, L.-S. *J. Organomet. Chem.* 1989, 377, C59. (c) Bantel, H.; Powell, A. K.; Vahrenkamp, H. *Chem. Ber.* 1990, 123, 661. (d) Boyar, E.; Deeming, A. J.; Felix, M. S. B.; Kabir, S. E.; Adatia, T.; Bhusate, R.; McPartlin, M.; Powell, H. R. *J. Chem. Soc., Dalton Trans.* 1989, 5. (e) Grist, N. J.; Hogarth, G.; Knox, S. A. R.; Lloyd, B. R.; Morton, D. A. V.; Orpen, A. G. *J. Chem. Soc., Chem. Commun.* 1988, 673.

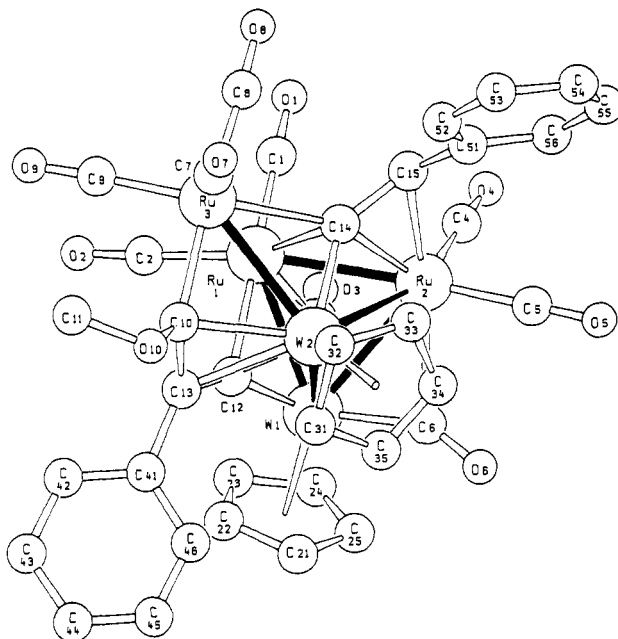
**Table VII. Selected Bond Distances (Å) and Angles (deg) for Complex 4 (Esd's in Parentheses)**

(A) Intermetallic Distances			
W(1)–W(2)	2.897 (1)	W(1)–Ru(1)	2.822 (2)
W(1)–Ru(2)	2.875 (2)	W(2)–Ru(1)	2.861 (1)
W(2)–Ru(2)	2.849 (2)	Ru(1)–Ru(2)	2.773 (2)
Ru(1)–Ru(3)	2.740 (2)	Ru(1)–Ru(3)	2.709 (2)
(B) Selected Parameters for the Carbonyl Ligands			
W(1)–C(1)	1.98 (2)	W(2)–C(2)	1.96 (2)
Ru(1)–C(2)	2.31 (2)	Ru(2)–C(2)	2.27 (2)
Ru(3)–C(2)	2.40 (2)	Ru(3)–O(2)	2.14 (1)
C(2)–O(2)	1.25 (2)	Ru(1)–C(3)	1.87 (2)
Ru(1)–C(4)	1.84 (2)	Ru(2)–C(5)	1.87 (2)
Ru(2)–C(6)	1.85 (3)	Ru(3)–C(7)	1.87 (2)
Ru(3)–C(8)	1.89 (2)	Ru(3)–C(9)	1.91 (3)
$\angle W(1)–C(1)–O(1)$	166 (2)	$\angle W(2)–C(2)–O(2)$	147 (1)
$\angle W(2)–C(2)–Ru(3)$	150.1 (8)	$\angle Ru(1)–C(2)–Ru(2)$	74.6 (5)
$\angle Ru(1)–C(3)–O(3)$	180 (2)	$\angle Ru(1)–C(4)–O(4)$	176 (2)
$\angle Ru(2)–C(5)–O(5)$	179 (2)	$\angle Ru(2)–C(6)–O(6)$	178 (2)
$\angle Ru(3)–C(7)–O(7)$	176 (2)	$\angle Ru(3)–C(8)–O(8)$	175 (3)
$\angle Ru(3)–C(9)–O(9)$	178 (2)		
(C) Parameters Associated with the Methylidyne Fragment			
W(1)–C(10)	2.21 (1)	W(2)–C(10)	1.99 (2)
Ru(1)–C(10)	2.13 (2)	C(10)–O(10)	1.36 (2)
C(11)–O(10)	1.44 (2)		
(D) Parameters Associated with the Acetylide Fragment			
W(1)–C(12)	2.23 (2)	W(2)–C(12)	2.01 (2)
Ru(2)–C(12)	2.21 (2)	W(1)–C(13)	2.18 (2)
Ru(2)–C(13)	2.21 (2)	C(12)–C(13)	1.27 (2)
$\angle W(2)–C(12)–C(13)$	151 (1)	$\angle C(12)–C(13)–C(21)$	139 (2)

3:1:1 serves as the strongest indication of the commencement of the internuclear exchange of the bridging CO and the CO ligands on both Ru(CO)<sub>2</sub> centers. Finally, at 355 K with toluene-d<sub>8</sub> as solvent, the <sup>13</sup>C NMR spectrum exhibits a sharp signal at  $\delta$  256.0 assigned to the immobile W–CO ligands and three broad signals in the region of Ru–CO resonances, indicating the beginning of rapid CO scrambling over all three ruthenium atoms. We attribute the high activation barrier of the complete CO scrambling over all three Ru centers with respect to the second process to be due to the absence of a bridging CO ligand on the Ru(1)–Ru(2) and Ru(1)–Ru(3) edges.<sup>13</sup>

**Reactivity of Complex 2.** After concluding the characterization of 2, we proceed to examine the reactivity of this new heterobimetallic cluster. Treatment of a toluene solution of 2 under carbon monoxide (1 atm, 28 °C) instantly changed the color from olive green to red, suggesting that complex 2 can create some vacant coordination site for the incoming carbon monoxide via cleavage of a metal–metal bond.<sup>14</sup> Unfortunately, the new complex is unstable in the absence of the atmosphere of carbon monoxide at room temperature. When a partial vacuum was applied above the solution, we saw an instantaneous color change from red to olive green, indicating the regeneration of 2. This preliminary reactivity study signifies that complex 2 is potentially unsaturated; therefore, it should react with the mononuclear building blocks, such as CpW(CO)<sub>3</sub>H and CpW(CO)<sub>3</sub>C≡CPh, to afford clusters with one additional transition-metal atom (Scheme I).

**Synthesis and Characterization of 3.** Treatment of complex 2 with 1 equiv of CpW(CO)<sub>3</sub>C≡CPh in toluene gave the brown complex Cp<sub>2</sub>W<sub>2</sub>Ru<sub>3</sub>(CO)<sub>9</sub>[CCPhC(OMe)](C=CHPh) (3) in low yield. The structural formula of 3 was determined by FAB mass spectrometry which indicates a parent ion at *m/z* 1302, corresponding to the composition C<sub>37</sub>H<sub>24</sub>O<sub>10</sub>Ru<sub>3</sub>W<sub>2</sub>. This formulation

**Figure 3.** Molecular structure of Cp<sub>2</sub>W<sub>2</sub>Ru<sub>3</sub>(CO)<sub>9</sub>[CC(Ph)C(OMe)](C=CHPh) (3).

indicates that the formation of 3 involves the addition of one CpW(CO)<sub>3</sub>C≡CPh molecule accompanied by elimination of three CO ligands. The IR spectrum in cyclohexane exhibits five absorptions attributed to CO stretching at 2057, 2018, 2003, 1977, and 1967 cm<sup>-1</sup>. The <sup>1</sup>H NMR spectrum shows two sets of phenyl resonances in the region  $\delta$  7.52–7.02, a vinylidene  $\beta$ -hydrogen resonance at  $\delta$  7.47, two Cp resonances at  $\delta$  5.37 and 4.64, and a methyl resonance at  $\delta$  3.93, confirming the formulation established by FAB mass spectrometry. Finally, the unambiguous molecular structure was determined by single-crystal X-ray diffraction analysis.

**Crystal Structure of Complex 3.** Dark brown crystals of 3 suitable for X-ray structural analysis were obtained from a solution of dichloromethane and hexane at room temperature. The molecular geometry and atomic labeling scheme are shown in Figure 3, and important bond distances and angles are listed in Table V. The molecule possesses a Ru<sub>3</sub>W<sub>2</sub> core structure, which can be considered to adopt an edge-bridged tetrahedral configuration,<sup>15</sup> as expected for an M<sub>5</sub> cluster species characterized by 74 valence electrons.<sup>16</sup> The atoms W(1), W(2), Ru(1), and Ru(2) define the required tetrahedral arrangement in which both ruthenium atoms of this Ru<sub>2</sub>W<sub>2</sub> tetrahedral core are linked to two terminal CO ligands, while atom W(1) is linked to a Cp and two CO ligands and atom W(2) is capped by a Cp ligand, respectively. In addition, the edge-bridged ruthenium atom Ru(3) is coordinated to the W(2)–Ru(1) vector of the Ru<sub>3</sub>W<sub>2</sub> core arrangement and is also coordinated by three CO ligands. The dihedral angle between the triangular planes W(2)–Ru(1)–Ru(3) and W(1)–W(2)–Ru(1) is 161.2°, and the lengths of the metal–metal bonds in this molecule are normal and lie within the expected range 3.1138 (6)–2.7388 (8) Å. All CO ligands on ruthenium atoms are effectively linear with M–C–O angles ranging from 176.3 (6) to 179.6 (6)°, whereas the two CO ligands on the atom W(1) are bent with angles  $\angle W(1)–C(3)–O(3) = 153.4 (5)^\circ$  and  $\angle W(1)–C(6)–O(6) = 149.6 (6)^\circ$ . Therefore, these W–CO ligands can be con-

(13) Band, E.; Muettterties, E. L. *Chem. Rev.* 1978, 78, 639.

(14) Chi, Y.; Chuang, S.-H.; Liu, L.-K. Unpublished results.

(15) Sappa, E.; Tiripicchio, A.; Carty, A. J.; Toogood, G. E. *Prog. Inorg. Chem.* 1987, 35, 437.(16) Mingos, D. M. P. *Acc. Chem. Res.* 1984, 17, 311.

sidered to be semibridging CO ligands.

In addition to the CO ligands, there are two coordinated hydrocarbon fragments on the ligand sphere of the  $\text{Ru}_3\text{W}_2$  framework. The  $\text{C}_3$  hydrocarbon fragment  $\text{CC}(\text{Ph})\text{C}(\text{OMe})$  is derived from the coupling of the acetylide of  $\text{CpW}(\text{CO})_3\text{C}\equiv\text{CPh}$  and the methoxymethylidyne ligand of **2**, occupying the face of a flat butterfly arrangement with  $\text{Ru}(1)$  and  $\text{W}(2)$  located on the hinge positions and  $\text{W}(1)$  and  $\text{Ru}(3)$  on the wingtip positions. The bonding of this  $\text{C}_3$  hydrocarbon fragment is exceptional, in that the  $\text{CC}(\text{Ph})\text{C}(\text{OMe})$  unit supplies three electrons to the atom  $\text{W}(2)$  and a total of six electrons to the cluster. In addition, because the bond distances  $\text{W}(2)\text{--C}(10) = 2.282$  (6) Å and  $\text{W}(2)\text{--C}(13) = 2.344$  (6) Å are the longest metal–carbon distances within this  $\text{C}_3$  fragment, we can visualize that the  $\text{C}(10)\text{--C}(13)$  linkage is in fact coordinated to the atom  $\text{W}(2)$  via a regular  $\pi$ -bonding interaction (Scheme I). Thus, this  $\text{C}_3$  hydrocarbon is a substituted triply bridging alkylidyne, in which the  $\alpha$ -carbon  $\text{C}(12)$  is linked to metal atoms  $\text{W}(1)$ ,  $\text{W}(2)$ , and  $\text{Ru}(1)$  via three  $\sigma$ -bonds and the pendant  $\text{C}_2$  substituent ( $\text{C}(10)\text{--C}(13)$ ) is  $\sigma$ -bonded to  $\text{Ru}(3)$  and  $\pi$ -bonded to the  $\text{W}(2)$  atom. Alternatively, as indicated by a reviewer, this  $\text{C}_3$  fragment can also be considered as a trimetallaallyl ligand coordinated to  $\text{W}(2)$ , because the  $\text{C}(10)\text{--C}(13)$  bond is longer than the  $\text{C}(12)\text{--C}(13)$  bond. This description is in accord with that of the dimetallaallyl fragment observed in systems of trinuclear complexes.<sup>17</sup> However, we cannot find any trimetallaallyl complexes in the literature for comparison.

The second hydrocarbon fragment is a vinylidene ( $\text{C}=\text{CHPh}$ ) fragment, which lies on the face of another butterfly arrangement defined by the atoms  $\text{W}(2)$ ,  $\text{Ru}(1)$ ,  $\text{Ru}(2)$ , and  $\text{Ru}(3)$ . The dihedral angle between the triangular planes  $\text{W}(2)\text{--Ru}(1)\text{--Ru}(2)$  and  $\text{W}(2)\text{--Ru}(1)\text{--Ru}(3)$  is  $130.4^\circ$ . The  $\alpha$ -carbon of the vinylidene is connected to all the metal atoms with  $\text{W}(2)\text{--C}(14) = 2.009$  (6) Å,  $\text{Ru}(1)\text{--C}(14) = 2.139$  (5) Å,  $\text{Ru}(2)\text{--C}(14) = 2.222$  (6) Å, and  $\text{Ru}(3)\text{--C}(14) = 2.365$  (6) Å, and the  $\beta$ -carbon is linked to the atom  $\text{Ru}(3)$  with  $\text{Ru}(2)\text{--C}(15) = 2.201$  (6) Å. On the basis of these structural data, we conclude that the vinylidene ligand adopts a novel  $\mu_4\text{-}\eta^2$ -bonding mode. To our knowledge, complex **3** is the fourth example in the literature to display a bonding interaction of this type.<sup>18</sup>

**Synthesis and Characterization of 4.** Reaction with  $\text{CpW}(\text{CO})_3\text{H}$  was carried out under slightly different reaction conditions. The successful synthesis of **4** depends on the careful control of the concentration of  $\text{CpW}(\text{CO})_3\text{H}$  in the solution. When a solution of complex **2** and 2 molar equiv of  $\text{CpW}(\text{CO})_3\text{H}$  was refluxed in toluene for 2 h, we failed to isolate any new complex but instead induced decomposition. However, the synthesis was improved by decreasing the effective concentration of  $\text{CpW}(\text{CO})_3\text{H}$  in the solution by means of dropwise addition of the  $\text{CpW}(\text{CO})_3\text{H}$  solution to the solution of **2** at reflux. Under these revised reaction conditions, we isolated the acetylide complex  $\text{Cp}_2\text{W}_2\text{Ru}_3(\text{CO})_9(\mu_3\text{-COMe})(\text{C}\equiv\text{CPh})$  (**4**) in 24% yield (Scheme I). The complex **4** was fully characterized by microanalysis, FAB mass spectrometry  $^1\text{H}$  NMR and IR spectroscopy and an X-ray structural determination. The  $^1\text{H}$  NMR spectrum exhibits a set of phenyl resonances, two Cp signals at  $\delta$  6.12 and 5.21, and a methyl resonance

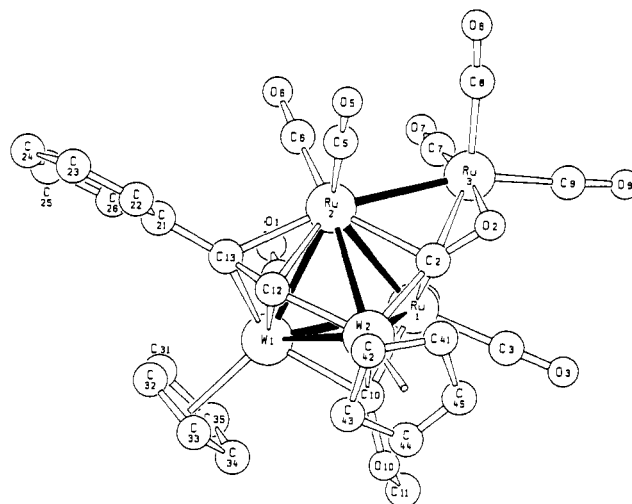


Figure 4. Molecular structure of  $\text{Cp}_2\text{W}_2\text{Ru}_3(\text{CO})_9(\mu_3\text{-COMe})(\text{C}\equiv\text{CPh})$  (**4**).

at  $\delta$  3.69, confirming the removal of the vinylidene  $\beta$ -hydrogen.

**Crystal Structure of Complex 4.** Red crystals of **4** suitable for X-ray diffraction were obtained from a layered solution of dichloromethane and methanol at room temperature. The molecule crystallizes in the monoclinic space group  $P2_1/c$  with the presence of one water molecule in the unit cell. There are no uncommon intermolecular contacts between individual molecules in the crystal. The geometry and atomic labeling scheme are presented in Figure 4, and selected interatomic distances and angles are collected in Table VII.

The  $\text{Ru}_3\text{W}_2$  core arrangement of this complex also adopts an edge-bridged tetrahedral geometry as expected for the  $\text{M}_5$  cluster species characterized by 74 valence electrons. Atoms  $\text{W}(1)$ ,  $\text{W}(2)$ ,  $\text{Ru}(1)$ , and  $\text{Ru}(2)$  define the basic tetrahedral core arrangement in which each ruthenium atom is connected to two CO ligands, the  $\text{W}(1)$  atom is capped by Cp and CO ligands, and the  $\text{W}(2)$  atom is coordinated to a Cp ligand, respectively. The edge-bridged metal atom  $\text{Ru}(3)$  is located on the edge of the  $\text{Ru}(1)\text{--Ru}(2)$  vector of the  $\text{Ru}_2\text{W}_2$  tetrahedral core and is also linked by three CO ligands. The distances of all metal–metal bonds are in the normal range of metal–metal single bonds (2.709 (2)–2.897 (1) Å). The dihedral angles between the planes  $\text{Ru}(1)\text{--Ru}(2)\text{--Ru}(3)$  and  $\text{W}(2)\text{--Ru}(1)\text{--Ru}(2)$  and between the planes  $\text{Ru}(1)\text{--Ru}(2)\text{--Ru}(3)$  and  $\text{W}(1)\text{--Ru}(1)\text{--Ru}(2)$  are  $134.8$  and  $172.5^\circ$ , respectively. Formal electron counts at the individual metal atoms are 17 e at  $\text{W}(2)$ , 18 e at  $\text{Ru}(1)$ ,  $\text{Ru}(2)$ , and  $\text{Ru}(3)$ , and 19 e at  $\text{W}(1)$ .

In addition to the CO ligands, there are two hydrocarbon fragments in the ligand sphere. The first one is a  $\text{C}_2$  acetylide fragment,  $\text{C}(12)\text{--C}(13)$ , which occupies the  $\text{W}(1)\text{--W}(2)\text{--Ru}(2)$  face with its  $\alpha$ -carbon bound to all three metal atoms and with its  $\beta$ -carbon linked to the atoms  $\text{W}(1)$  and  $\text{Ru}(2)$ . This acetylide is considered to adopt a  $1\sigma + 2\pi$  interaction and donates a total of five electrons to the cluster.<sup>9</sup> Its local arrangement (perpendicular to one M–M bond) and the M–C distances associated with the acetylide ligand ( $\text{W}(1)\text{--C}(12)$ , 2.23 (2) Å;  $\text{W}(2)\text{--C}(12)$ , 2.01 (2) Å;  $\text{Ru}(2)\text{--C}(12)$ , 2.21 (2) Å;  $\text{W}(1)\text{--C}(13)$ , 2.18 (2) Å) are in agreement with those observed for acetylide complexes such as  $\text{HO}_3(\text{CO})_9(\text{C}\equiv\text{CCF}_3)$ ,<sup>19</sup>  $\text{CpWRu}_2(\text{CO})_8(\text{C}\equiv\text{CPh})$ ,<sup>20</sup>  $\text{HRu}_3(\text{CO})_9(\text{C}\equiv\text{CBu}^t)$ ,<sup>21</sup> and  $\text{CoFe}_2$

(17) (a) Nuel, D.; Dahan, F.; Mathieu, R. *J. Am. Chem. Soc.* **1985**, *107*, 1658. (b) Lentz, D.; Michael-Schulz, H. *Inorg. Chem.* **1990**, *29*, 4396 and references cited therein.

(18) (a) Carty, A. J.; Taylor, N. J.; Sappa, E.; Tiripicchio, A. *Inorg. Chem.* **1983**, *22*, 1871. (b) Brun, A.; Dawkins, G. M.; Green, M.; Mills, R. M.; Salaün, J. Y.; Stone, F. G. A.; Woodward, P. *J. Chem. Soc., Dalton Trans.* **1983**, 1357. (c) Jeffery, J. C.; Johnson, B. F. G.; Lewis, J.; Raithby, P. R.; Welch, D. A. *J. Chem. Soc., Chem. Commun.* **1986**, 318.

(19) Dawoodi, Z.; Mays, M. J.; Henrich, K. *J. Chem. Soc., Dalton Trans.* **1984**, 1769.

(CO)<sub>9</sub>(C≡CSiMe<sub>3</sub>).<sup>22</sup> Furthermore, the second fragment is a methylidyne ligand, which is located on the adjacent W<sub>2</sub>Ru triangle with metal-carbon distances W(1)-C(10) = 2.21 (1) Å, W(2)-C(10) = 1.99 (2) Å, and Ru(1)-C(10) = 2.13 (2) Å. Its configuration is unremarkable, resembling that of its precursor 2.

The most striking feature is the presence of a quadruply bridging  $\mu_4\text{-}\eta^2\text{-CO}$  ligand,<sup>23</sup> which is encapsulated in the cavity of the Ru<sub>3</sub>W butterfly arrangement with metal-carbon distances W(2)-C(2) = 1.96 (2) Å, Ru(1)-C(2) = 2.31 (2) Å, Ru(2)-C(2) = 2.27 (2) Å, and Ru(3)-C(2) = 2.40 (2) Å and with angles  $\angle$ W(2)-C(2)-Ru(3) = 150.1 (8)° and  $\angle$ Ru(1)-C(2)-Ru(2) = 74.6 (5)°. The C-O distance of this carbonyl ligand (1.25 (2) Å) is substantially longer than the average distance of the ruthenium-bound terminal CO ligands in the molecule (1.14 Å), suggesting a weakening of the carbon-oxygen bond due to the donation of two extra  $\pi$ -electrons to the cluster. In addition, the oxygen atom is tilted away from the electropositive transition-metal atom W(2) and connected to the less electropositive Ru(3) atom with distance Ru(3)-O(2) = 2.14 (1) Å. The preference observed is consistent with that of the  $\mu_4\text{-}\eta^2\text{-CO}$  ligand in the WRu<sub>3</sub> complexes reported earlier.<sup>24</sup> Clearly, the relative electron affinity of the transition-metal atoms is not the only factor to determine the preference of the oxygen atom of the quadruply bridging CO ligand.

**Conclusion.** In summary, the reaction of complex 1 and CpW(CO)<sub>3</sub>C≡CPh provides a convenient entry to the new Ru<sub>3</sub>W cluster complex 2. This condensation reaction is in contrast with the corresponding reaction with the "organic acetylide", for which the coupling of the alkyne and alkylidyne ligands was observed. To explain the formation of complex 2, it is postulated that the reaction proceeds via addition of the bridging hydride of 1 across the C-C triple bond of CpW(CO)<sub>3</sub>C≡CPh, followed by formation of three new W-Ru bonds to build the tetrahedral cluster core via CO elimination. The formation of doubly bridging vinylidene ligands from the reaction between metal acetylides and hydrides is precedented.<sup>25</sup>

A variable-temperature <sup>13</sup>C NMR study suggests that the CO ligands on the ruthenium atoms of complex 2 in solution undergo both intranuclear and internuclear CO exchanges. The 3-fold rotation of the Ru(CO)<sub>3</sub> vertex and the intranuclear exchange between the bridging CO and the terminal CO on one of the adjacent Ru(CO)<sub>2</sub> vertices

are the two processes with the lowest activation barriers. While the temperature was increased to 294 K, we observed the internuclear CO exchange between the bridging and the four terminal CO ligands on both adjacent Ru(CO)<sub>2</sub> centers. Finally, above 355 K scrambling of all ruthenium CO ligands was noticed on the basis of the NMR line-shape analysis.

With regard to the reactivity studies, complex 2 is also an excellent starting material for making interesting polynuclear cluster complexes. The thermal condensation of 2 with the metal acetylide CpW(CO)<sub>3</sub>C≡CPh afforded complex 3 in moderate yield. The formation of 3 is best rationalized in terms of the coupling between the acetylide of CpW(CO)<sub>3</sub>C≡CPh and the methylidyne ligand of 2, which led to the generation of the observed C<sub>3</sub> alkylidyne fragment CC(Ph)=C(OMe). At the same time, the bonding of the vinylidene ligand changes from a triply bridging mode ( $\mu_3\text{-}\eta^2$ ) to a quadruply bridging mode ( $\mu_4\text{-}\eta^2$ ). The coupling of the acetylide and the methoxymethylidyne ligand is consistent with that of the reaction with several trinuclear methylidyne complexes: HRu<sub>3</sub>(CO)<sub>10</sub>( $\mu\text{-COMe}$ ) or H<sub>3</sub>Ru<sub>3</sub>(CO)<sub>9</sub>( $\mu_3\text{-COMe}$ )<sup>4</sup> and Fe<sub>3</sub>(CO)<sub>9</sub>( $\mu_3\text{-CMe}$ )( $\mu\text{-COEt}$ ).<sup>17</sup>

On the other hand, reaction with the metal hydride CpW(CO)<sub>3</sub>H proceeded via the similar pathway of cluster condensation, which increases the number of transition-metal atoms by one and also induces dehydrogenation of the vinylidene ligand on the ligand sphere of the newly assembled Ru<sub>3</sub>W<sub>2</sub> cluster core. In general, dehydrogenation of vinylidene is accomplished by addition of a hydrogen acceptor, such as alkyne, to the triosmium vinylidene complexes Os<sub>3</sub>(CO)<sub>9</sub>( $\mu\text{-H}$ )(CCHR) and Os<sub>3</sub>(CO)<sub>9</sub>( $\mu\text{-Br}$ )(CCHPh).<sup>26</sup> In contrast, the alkylidyne is the expected final product of the hydrogenation reaction and the addition of hydride or proton moieties to the vinylidene.<sup>27</sup> Thus, our result represents a rare case in which the transformation from vinylidene to acetylide is executed by addition of a metal hydride, which serves as the ultimate hydrogen acceptor. Finally, the structural determination of 4 indicates the existence of a quadruply bridging CO ligand. Its formation compensates for the unsaturation generated by elimination of hydride ligands in the intermediate containing two hydride ligands and one acetylide ligand. The reversible rearrangement between cluster-bound vinylidene and hydride-acetylide species has been reported for W<sub>2</sub>Os<sub>2</sub> complexes.<sup>28</sup>

**Acknowledgment.** We are grateful to the National Science Council of the Republic of China for financial support (Grant No. NSC80-0208-M007-60).

**Supplementary Material Available:** Tables of nonessential bond distances and angles, calculated positions of hydrogen atoms, and anisotropic thermal parameters for complexes 2-4 (17 pages); listings of observed and calculated structure factors (51 pages). Ordering information is given on any current masthead page.

(20) Hwang, D.-K.; Chi, Y.; Peng, S.-M.; Lee, G.-H. *Organometallics* 1990, 9, 2709.

(21) Catti, M.; Gervasio, G.; Mason, S. A. *J. Chem. Soc., Dalton Trans.* 1977, 2260.

(22) Seyferth, D.; Hoke, J. B.; Rheingold, A. L.; Cowie, M.; Hunter, A. D. *Organometallics* 1988, 7, 2163.

(23) (a) Horwitz, C. P.; Shriver, D. F. *Adv. Organomet. Chem.* 1984, 23, 219. (b) Manassero, M.; Sansoni, M.; Longoni, G. *J. Chem. Soc., Chem. Commun.* 1976, 919. (c) Brun, L. P.; Dawkins, G. M.; Green, M.; Miles, A. D.; Orpen, A. G.; Stone, F. G. A. *J. Chem. Soc., Chem. Commun.* 1982, 926. (d) Field, J. S.; Haines, R. J.; Jay, J. A. *J. Organomet. Chem.* 1989, 377, C35. (e) Adams, R. D.; Babin, J. E.; Tasi, M. *Inorg. Chem.* 1988, 27, 2618. (f) Horwitz, C. P.; Holt, E.; Brock, C. P.; Shriver, D. F. *J. Am. Chem. Soc.* 1985, 107, 8139. (g) Anson, C. E.; Bailey, P. J.; Conole, G.; Johnson, B. F. G.; Lewis, J.; McPartlin, M.; Powell, H. R. *J. Chem. Soc., Chem. Commun.* 1990, 442.

(24) Chi, Y.; Wu, F.-J.; Liu, B.-J.; Wang, C.-C.; Wang, S.-L. *J. Chem. Soc., Chem. Commun.* 1989, 873.

(25) Afzal, D.; Lenhart, P. G.; Lukehart, C. M. *J. Am. Chem. Soc.* 1984, 106, 3050.

(26) (a) Jackson, W. G.; Johnson, B. F. G.; Kelland, J. W.; Lewis, J.; Schorpp, K. T. *J. Organomet. Chem.* 1975, 87, C27. (b) Chi, Y.; Chen, B.-F.; Wang, S.-L.; Chiang, R.-K.; Hwang, L.-S. *J. Organomet. Chem.* 1989, 377, C59.

(27) Dutta, T. K.; Vites, J. C.; Fehlner, T. P. *Organometallics* 1986, 5, 385.

(28) Chi, Y.; Wu, C.-H.; Peng, S.-H.; Lee, G.-H. *Organometallics*, in press.